they may induce terminal differentiation of certain cell types. These are consistent with the previous observation that Ski and SnoN induce oncogenic transformation and muscle differentiation of quail embryo cells.

References and Notes

1. C.-H. Heldin, K. Miyazono, P. ten Dijke, *Nature* **390**, 465 (1997); J. Massague, *Annu. Rev. Biochem.* **67**, 753 (1998).
2. J. C. Baker and R. M. Harland, *Genes Dev.* **10**, 1880 (1996); P. A. Hoodless *et al.*, *Cell* **85**, 489 (1996).
3. F. Liu *et al.*, *Nature* **381**, 620 (1996).
4. X. Liu *et al.*, *Proc. Natl. Acad. Sci. U.S.A.* **94**, 10669 (1997).
5. Y. Zhang, T. Musci, R. Derynck, *Curr. Biol.* **7**, 270 (1997).
6. M. S. Macias-Silva *et al.*, *Cell* **87**, 1215 (1996); S. Abdollah *et al.*, *J. Biol. Chem.* **272**, 27678 (1997); M. P. de Caestecker *et al.*, *ibid.*, p. 13690; A. Nakao *et al.*, *ibid.*, p. 2896; S. Souchelnytskyi *et al.*, *ibid.*, p. 28107; Y. Zhang, X. Feng, R. Wu, R. Derynck, *Nature* **383**, 168 (1996).
7. G. Lagna, A. Hata, A. Hemmati-Brivanlou, J. Massague, *Nature* **383**, 832 (1996); R. Y. Wu, Y. Zhang, X. H. Feng, R. Derynck, *Mol. Cell. Biol.* **17**, 2521 (1997); Y. Shi, A. Hata, R. S. Lo, J. Massague, N. P. Pavletich, *Nature* **388**, 87 (1997).
8. X. Chen, M. J. Rubock, M. Whitman, *Nature* **383**, 691 (1996); X. Chen *et al.*, *ibid.* **389**, 85 (1997); E. Labbe, C. Silvestri, P. A. Hoodless, J. L. Wrana, L. Attisano, *Mol. Cell* **2**, 109 (1998); X.-H. Feng, Y. Zhang, R.-Y. Wu, R. Derynck, *Genes. Dev.* **12**, 2153 (1998); R. Janknecht, N. J. Wells, T. Hunter, *ibid.*, p. 2114; C. Pouponnot, L. Jayaraman, J. Massague, *J. Biol. Chem.* **273**, 22865 (1998); X. Shen *et al.*, *Mol. Biol. Cell* **9**, 3309 (1998); J. N. Topper *et al.*, *Proc. Natl. Acad. Sci. U.S.A.* **95**, 9506 (1998); C. Wong *et al.*, *Mol. Cell. Biol.* **19**, 1821 (1999); Y. Zhang, X.-H. Feng, R. Derynck, *Nature* **394**, 909 (1998); A. Moustakas and D. Kardassis, *Proc. Natl. Acad. Sci. U.S.A.* **95**, 6733 (1998).
9. S. Dennler *et al.*, *EMBO J.* **17**, 3091 (1998); S. Dennler, S. Huet, J. M. Gauthier, *Oncogene* **18**, 1643 (1999); L. J. Jonk, S. Itoh, C. H. Heldin, P. ten Dijke, W. Kruijer, *J. Biol. Chem.* **273**, 21145 (1998); Y. Shi *et al.*, *Cell* **94**, 585 (1998); C.-Z. Song, T. E. Siok, T. D. Gelehrter, *J.. Biol. Chem.* **273**, 29287 (1998); L. Vindevoghel *et al.*, *ibid.*, p. 13053; J. M. Yingling *et al.*, *Mol. Cell. Biol.* **17**, 7019 (1997).
10. S. L. Stroschein, W. Wang, K. Luo, *J. Biol. Chem.* **274**, 9431 (1999).
11. L. Zawel *et al.*, *Mol. Cell* **1**, 611 (1998).
12. Q. Zhou, D. Chen, E. Pierstorff, K. Luo, *EMBO J.* **17**, 3681 (1998).
13. Flag-tagged full-length Smad4, Smad4C (residues 319 to 551), or Smad4NL (residues 1 to 318) were transfected into 293T cells by the Lipofectamine-Plus method (Gibco-BRL). Stable 293T cells expressing Flag-Smad4C were generated by cotransfecting pCMV5B-Flag-Smad4C with a construct expressing the puromycin resistance gene, followed by selection in the presence of puromycin (1 μg/ml, Sigma). For large-scale purification of Smad4C-associated proteins, 2×10^9 cells were lysed in buffer containing 50 mM Hepes (pH 7.8), 500 mM NaCl, 5 mM EDTA, 1% Nonidet P-40, 3 mM dithiothreitol, and 0.5 mM phenylmethylsulfonyl fluoride. Lysates were then applied to anti-Flag M2 agarose (Sigma) (30 μl of anti-Flag agarose per milliliter of lysate). After extensive washing, Smad4C and its associated proteins were eluted with Flag peptide (0.4 mg/ml) (*12*). The proteins were resolved on a 10% low-Bis polyacrylamide gel, transferred to nitrocellulose membrane, and digested with Lys-C. Five peptides from the 80-kD protein were sequenced and showed a perfect match to c-SnoN: KIILEEMK (amino acid residues 345 to 452 in SnoN), KTDAPSGMELQS (residues 366 to 377), KTVSYPDVSLEE (residues 449 to 460), KVGIGLVAAASS (residues 503 to 514), and KLEMMIK (residues 663 to 669). Abbreviations for the amino acid residues are as follows: A, Ala; D, Asp; E, Glu; G, Gly; I, Ile; K, Lys; L, Leu; M, Met; P, Pro; Q, Gln; S, Ser; T, Thr; V, Val; and Y, Tyr.
14. S. L. Stroschein and K. Luo, data not shown.
15. N. Nomura *et al.*, *Nucleic Acids Res.* **17**, 5489 (1989).
16. K. Luo *et al.*, *Genes Dev.* **13**, 2196 (1999).
17. Y. Li, C. M. Turck, J. K. Teumer, E. Stavnezer, *J. Virol.* **57**, 1065 (1986); E. Stavnezer, A. E. Barkas, L. A. Brennan, D. Brodeur, Y. Li, *ibid.*, p. 1073.
18. S. Pearson-White, *Nucleic Acids Res.* **21**, 4632 (1993); _____ and R. Crittenden, *ibid.* **25**, 2930 (1997).
19. P. L. Boyer, C. Colmenares, E. Stavnezer, S. H. Hughes, *Oncogene* **8**, 457 (1993).
20. T. Nomura *et al.*, *Genes Dev.* **13**, 412 (1999).
21. S. B. Cohen, R. Nicol, E. Stavnezer, *Oncogene* **17**, 2505 (1998).
22. Supplemental information is available at *Science* Online at www.sciencemag.org/feature/data/1042351.shl.
23. L. Alland *et al.*, *Nature* **387**, 49 (1997); T. Heinzel *et al.*, *ibid.*, p. 43.
24. To measure the half-life of SnoN, transfected 293T cells were pulsed for 30 min in the presence of ^{35}S-express (0.25 mCi/ml, NEN) and chased for various periods of time as indicated in Fig. 3B. Cells were then lysed and SnoN isolated by immunoprecipitation.
25. To generate stable murine Ba/F3 cell lines overexpressing SnoN, Flag-SnoN was cloned into the retroviral vector pMX-IRES-GFP (*4*) that also expresses green fluorescence protein (GFP). The construct was used to transfect Bing cells to generate amphotropic retroviruses expressing Flag-SnoN. Forty-eight hours after transfection, 1×10^7 Ba/F3 cells were cocultivated with the transfected Bing cells for 24 hours, and the infected cells were selected by cell sorting on the basis of GFP expression.
26. R. Dahl, M. Kieslinger, H. Beug, M. J. Hayman, *Proc. Natl. Acad. Sci. U.S.A.* **95**, 11187 (1998).
27. K. A. W. Lee, A. Bindereif, M. R. Green, *Genet. Anal. Tech.* **5**, 22 (1987).
28. Two polyclonal antibodies to SnoN were raised, one against a glutathione-*S*-transferase (GST) fusion protein containing residues 1 to 366 of the human SnoN protein [antibody (Ab) 1330], and the other against a peptide located at the COOH-terminus of human SnoN (KELKLQILKSSKTAKE). For immunoprecipitation of endogenous SnoN, the peptide antibody was covalently coupled to protein A Sepharose and incubated with lysates from Hep3B cells stimulated with or without TGF-β1. SnoN bound to the antibody column was then eluted with an excess amount of immunizing peptide and analyzed by protein immunoblotting with anti-Smad4 (Santa Cruz) or with anti-SnoN (Ab 1330).

29. We thank S. Pearson-White for providing the c-snoN cDNA, P. Kaufman for the human CAC1 probe, and H. Nolla for help with the FACS analysis. Supported by U.S. Department of Energy (DOE)–LBNL grant DE-AC03-76SF00098, DOE/OBER grant DE-AC03-76SF00099, Wendy Will Case Cancer Fund, California breast cancer research program award, and March of Dimes research grant to K.L. S.L.S. was supported by a predoctoral fellowship from the National Science Foundation.

3 June 1999; accepted 28 September 1999

Aging-Dependent Large Accumulation of Point Mutations in the Human mtDNA Control Region for Replication

Yuichi Michikawa,[1] Franca Mazzucchelli,[2] Nereo Bresolin,[2] Guglielmo Scarlato,[2] Giuseppe Attardi*[1]

Progressive damage to mitochondrial DNA (mtDNA) during life is thought to contribute to aging processes. However, this idea has been difficult to reconcile with the small fraction of mtDNA so far found to be altered. Here, examination of mtDNA revealed high copy point mutations at specific positions in the control region for replication of human fibroblast mtDNA from normal old, but not young, individuals. Furthermore, in longitudinal studies, one or more mutations appeared in an individual only at an advanced age. Some mutations appeared in more than one individual. Most strikingly, a T414G transversion was found, in a generally high proportion (up to 50 percent) of mtDNA molecules, in 8 of 14 individuals above 65 years of age (57 percent) but was absent in 13 younger individuals.

One postulated cause of aging is the accumulation of mutations in mtDNA (*1*). This notion is supported by the observation of an aging-related accumulation in human mtDNA of oxidative and alkylation derivatives of nucleotides (*2*), of small deletions and insertions (*2*), and of large deletions (*3*), although their low frequency (<1 to 2%) has raised questions about their functional significance. Furthermore, it has not been clear whether there is an accumulation of aging-dependent point mutations in human mtDNA (*4*), due in part to the lack of a reliable method for detecting heteroplasmic mutations (that is, mutations that occur together with wild-type mtDNA) and to the search having been largely limited to the protein- and RNA-coding regions of mtDNA.

[1]Division of Biology, California Institute of Technology, Pasadena, CA 91125, USA. [2]University of Milan, Institute of Clinical Neurology, Dino Ferrari Center, IRCCS, and Ospedale Maggiore di Milano–Policlinico, IRCCS E. Medea–Bosisio Parini (LC), 20122 Milan, Italy.

*To whom correspondence should be addressed. E-mail: attardig@seqaxp.bio.caltech.edu

The main control region of mtDNA [the D-loop and adjacent transcription promoters (DLP) (*5*)] is the most variable portion of the human mitochondrial genome (*6*) and may contain heteroplasmic point mutations (*7*). We therefore analyzed the mtDNA control region with a sensitive method for detection of aging-related heteroplasmic mutations. This approach, which allows the identification of as few as 2 to 4% point mutations while excluding false positives from nuclear mtDNA pseudogenes (*8*), is based on the use of mtDNA highly purified by cell fractionation and enzyme digestion and of a sensitive technique—denaturant gradient gel electrophoresis (DGGE)—that can identify single-nucleotide mismatches in artificially produced heteroduplexes (*9*), in combination with cloning, second-round DGGE, and sequencing. The mtDNA-less cell line ρ^0 206 (*10*) was used as a negative control. For DGGE analysis, the main mtDNA control region was subdivided into seven segments, 160 to 440 base pairs in length (DLP1 to DLP7), each with a single uniform melting domain (Fig. 1A) (*11*). The two segments DLP4 and DLP6, which correspond to one of the hypervariable portions of the main control region (*12*), were used. DLP4 contains the primary origin of heavy (H)–strand mtDNA synthesis (O_{H_1}), while DLP6 contains the two evolutionarily conserved sequence blocks CSB2 and CSB3 (*13*) and the promoter and start site for light (L)–strand transcription and H-strand replication RNA primer synthesis (*14*). The block CSB2 carries the homopolymeric tract (HT) D310, a sequence of 12 to 18 Cs interrupted by a T at position 310 (*15*), which exhibits length variation among individuals (*12, 16*) and heteroplasmic variation within an individual (*7, 17*).

To evaluate the role of nuclear mtDNA pseudogenes in yielding polymerase chain reaction (PCR) products with mtDNA-specific primers, total DNA (*18*) from $\rho^0$206 cells was tested with primers specific for the mtDNA DLP4 and DLP6 segments, for two mitochondrial tRNA genes [$tRNA^{Phe}$, $tRNA^{Leu(UUR)}$], for the region containing the origin of mtDNA L-strand synthesis (O_L), and, as a control, for three nuclear genes [coding for the 28*S* rRNA, the p53, and the adenosine triphosphatase (ATPase) α-subunit (*19*)]. PCR products were obtained with primers for the three nuclear genes, with primers for the two mitochondrial tRNA genes, for O_L, and, in small amounts, for DLP4 (Fig. 1B, panel a). These results indicate the presence of nuclear pseudogenes corresponding to these mtDNA segments in $\rho^0$206 cells. Using as a template total DNA from $\rho^0$206 cells in which nuclear DNA and nucleo-cytosolic RNA had been nearly completely digested with Bgl II, Dra III, ribonuclease A (RNase A), and exonuclease III (Fig. 1C) (*20*), products were still obtained with the primers for the 28*S* rRNA, p53 and ATPase α-subunit genes, as well as for the two mitochondrial tRNA genes and O_L, but no products with the primers for DLP4 and DLP6 (Fig. 1B, panel b). In further tests, DNA extracted from the micrococcal nuclease-treated mitochondrial fraction of $\rho^0$206 cells (*18*) yielded products only with primers for the $tRNA^{Phe}$, p53 and 28*S* rRNA genes (Fig. 1B, panel c). After digestion with Bgl II, Dra III, and Exo III, the same DNA yielded only products of 28*S* rRNA genes, presumably reflecting the very large number of copies of these genes (Fig. 1B, panel d). MtDNA purified in the same way from fibroblasts of a 19-year-old individual also yielded, aside from the expected PCR amplification products of the five mtDNA segments tested, a small amount of 28*S* rRNA gene products (Fig. 1B, panel e). This purification method was used for all the analyses below.

The PCR products of the DLP4 and DLP6 segments of untreated total cell DNA and highly purified mtDNA from fibroblast cultures of 18 randomly chosen, genetically unrelated normal individuals between 20-week fetal (20 wf) and 101 years in age and of nine normal individuals twice-sampled, with a 9- to 19-year interval, for the Gerontology Research Center (National Institutes of Health) longitudinal study (LS), were subjected to first-DGGE analysis (*21, 22*). Figure 2A, panel a, shows the DLP4 profiles of highly purified mtDNA from representative fibroblast cultures, including the two LS5 samples; Fig. 2A, panels b and c, show the DLP6 profiles of untreated total cell DNA (b) or highly purified mtDNA (c) from the same fibroblast samples; and Fig. 2A, panel d, shows the DLP6 profiles of purified mtDNA from fibroblasts of the other eight LS individuals. The DLP4, and especially the DLP6 PCR products from old individuals (>65 y), showed a tendency to exhibit, besides the homoduplex band and a band corresponding to uncrosslinked molecules (UX), one or more slower migrating bands, indicative of sequence variants, which resulted from heteroduplex for-

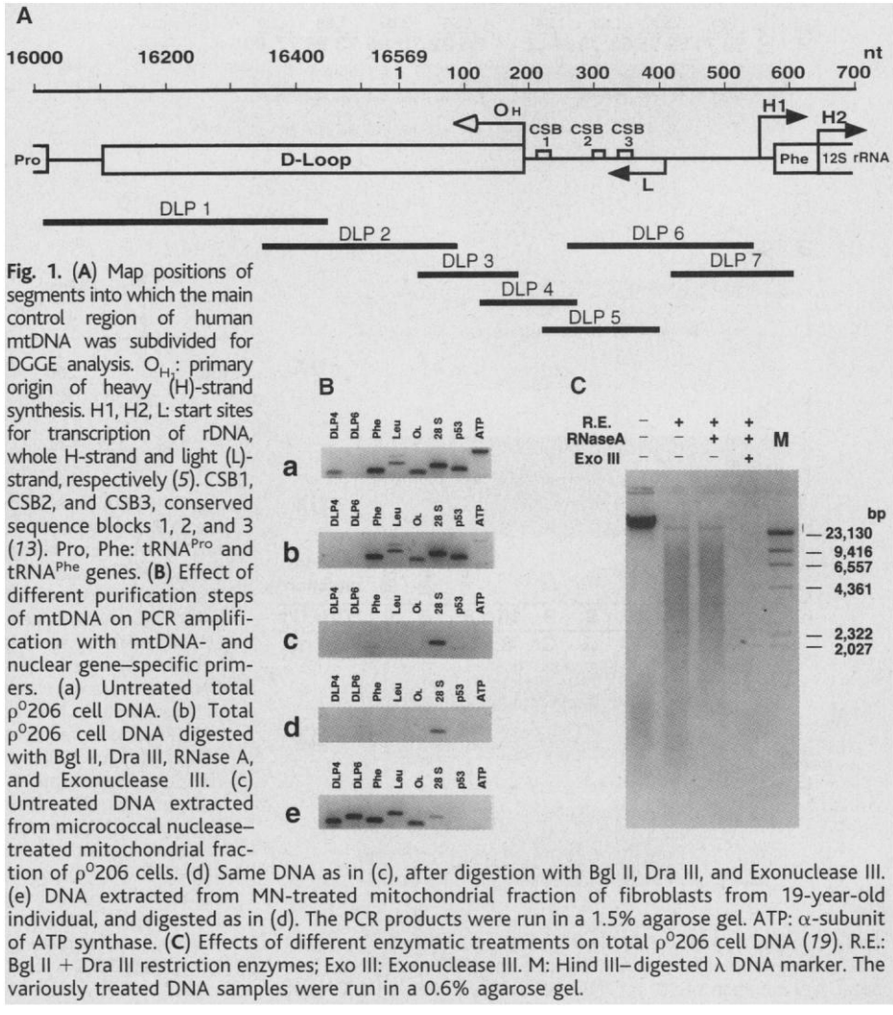

Fig. 1. (**A**) Map positions of segments into which the main control region of human mtDNA was subdivided for DGGE analysis. O_{H_1}: primary origin of heavy (H)-strand synthesis. H1, H2, L: start sites for transcription of rDNA, whole H-strand and light (L)-strand, respectively (*5*). CSB1, CSB2, and CSB3, conserved sequence blocks 1, 2, and 3 (*13*). Pro, Phe: $tRNA^{Pro}$ and $tRNA^{Phe}$ genes. (**B**) Effect of different purification steps of mtDNA on PCR amplification with mtDNA- and nuclear gene–specific primers. (a) Untreated total $\rho^0$206 cell DNA. (b) Total $\rho^0$206 cell DNA digested with Bgl II, Dra III, RNase A, and Exonuclease III. (c) Untreated DNA extracted from micrococcal nuclease–treated mitochondrial fraction of $\rho^0$206 cells. (d) Same DNA as in (c), after digestion with Bgl II, Dra III, and Exonuclease III. (e) DNA extracted from MN-treated mitochondrial fraction of fibroblasts from 19-year-old individual, and digested as in (d). The PCR products were run in a 1.5% agarose gel. ATP: α-subunit of ATP synthase. (**C**) Effects of different enzymatic treatments on total $\rho^0$206 cell DNA (*19*). R.E.: Bgl II + Dra III restriction enzymes; Exo III: Exonuclease III. M: Hind III–digested λ DNA marker. The variously treated DNA samples were run in a 0.6% agarose gel.

mation in the final melting and annealing steps (*9*). Especially significant is the fact that, in five of the nine LS sample pairs (LS1, LS4, LS6, LS7, and LS9), sequence variants of DLP6 appeared only, or were more diverse (in LS6), in the sample taken at a more advanced age.

After the first-DGGE assays, the PCR-amplified DLP6 fragments from nearly all purified mtDNA samples and all DLP4 fragments exhibiting abnormal bands were further analyzed. For this purpose, these fragments were cloned in *Escherichia coli*, and a large number of plasmids (in general, 42 to 48) were isolated from each source, and their DNAs were subjected to PCR amplification and a second-DGGE step, after hybridization with one of them randomly chosen as a reference clone (*23*). The possible patterns of homoduplexes or heteroduplexes, or both, expected in this hybridization step are illustrated schematically in Fig. 2B (*23*). All presumptive mutant clones and several of the presumptive wild-type clones identified by the second-DGGE analysis were then sequenced, together with one or more reference clones (*24*). Furthermore, the PCR-amplified

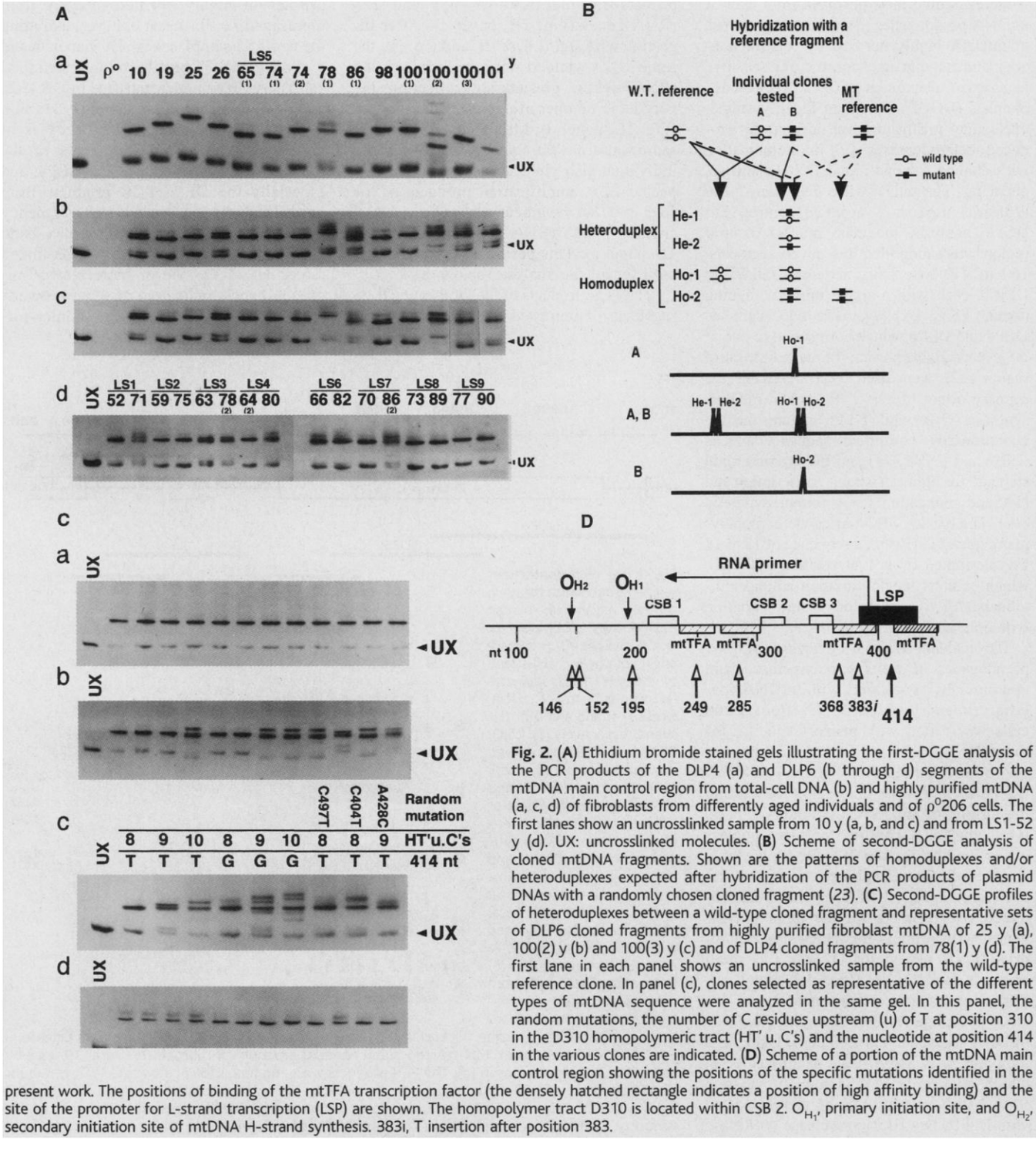

Fig. 2. (**A**) Ethidium bromide stained gels illustrating the first-DGGE analysis of the PCR products of the DLP4 (a) and DLP6 (b through d) segments of the mtDNA main control region from total-cell DNA (b) and highly purified mtDNA (a, c, d) of fibroblasts from differently aged individuals and of $\rho^0$206 cells. The first lanes show an uncrosslinked sample from 10 y (a, b, and c) and from LS1-52 y (d). UX: uncrosslinked molecules. (**B**) Scheme of second-DGGE analysis of cloned mtDNA fragments. Shown are the patterns of homoduplexes and/or heteroduplexes expected after hybridization of the PCR products of plasmid DNAs with a randomly chosen cloned fragment (*23*). (**C**) Second-DGGE profiles of heteroduplexes between a wild-type cloned fragment and representative sets of DLP6 cloned fragments from highly purified fibroblast mtDNA of 25 y (a), 100(2) y (b) and 100(3) y (c) and of DLP4 cloned fragments from 78(1) y (d). The first lane in each panel shows an uncrosslinked sample from the wild-type reference clone. In panel (c), clones selected as representative of the different types of mtDNA sequence were analyzed in the same gel. In this panel, the random mutations, the number of C residues upstream (u) of T at position 310 in the D310 homopolymeric tract (HT' u. C's) and the nucleotide at position 414 in the various clones are indicated. (**D**) Scheme of a portion of the mtDNA main control region showing the positions of the specific mutations identified in the present work. The positions of binding of the mtTFA transcription factor (the densely hatched rectangle indicates a position of high affinity binding) and the site of the promoter for L-strand transcription (LSP) are shown. The homopolymer tract D310 is located within CSB 2. O_{H_1}, primary initiation site, and O_{H_2}, secondary initiation site of mtDNA H-strand synthesis. 383i, T insertion after position 383.

DLP4 fragments of all individuals below 48 years in age were also directly sequenced.

Figure 2C shows second-DGGE profiles produced by heteroduplexes between wild-type mtDNA and representative sets of cloned DLP6 fragments from individuals of different ages: 25 y (panel a), 100(2) y (panel b) and 100(3) y (panel c), and of cloned DLP4 fragments from 78(1) y (panel d). These profiles illustrate the main patterns of heteroplasmic point-mutations that we detected.

Three main types of mutations were revealed by the sequence analysis (*25*): (i) specific point mutations, present in general in a high proportion of mtDNA molecules; (ii) length and sequence variations of the HT D310 and of a $(CA)_n$ repeat; and (iii) random point mutations. Two experiments aimed at estimating the background mtDNA sequence variation associated with the PCR and cloning steps [plasmid controls (*26*)] revealed a level of heteroplasmy of 0 and 2% (*25*).

We found an aging-related accumulation of high copy specific point mutations, almost always base substitutions, in the DLP6 region (Fig. 3). This was in contrast with the behavior of the HT D310 or (CA)n length variation, or of random single-base substitutions or deletions that were not restricted to old individuals (Fig. 3) (*25*). In fact, 170 of a total of 802 DLP6 plasmid clones derived from 10 of the 14 individuals older than 65 years carried a specific point mutation outside of HT D310. Between 5 and 50% of the clones from each individual contained mutations. In contrast, no such mutation was present in DLP6 in a total of 581 plasmid clones from 13 younger individuals (Fig. 3). Some mutations occurred in more than one individual. The most conspicuous example was a T414G transversion in DLP6 clones from fibroblasts of eight genetically unrelated individuals older than 65 y (Fig. 3) (*25*). No T414G transversion was found in the plasmid control. The mutations T414G, T285C, A368G, and T insertion after 383 were not previously reported (*27*).

Strong support for the age-dependency of the accumulation of specific point mutations in DLP6 was provided by the analysis of samples taken twice from the same individuals who were between 15 and 19 years apart in age. In three such studies, a specific mutation (A368G in LS1 and T414G in LS4 and LS7) was absent (LS1, LS4) or present at a marginal level (T414G in LS7) in the earlier sample, but was abundant (23 to 50%) in the later sample. In another study (LS6), the T414G transversion was found in a significant proportion of mtDNA in both the earlier and later samples, although considerably decreased in the latter (*28*). Two other LS studies (LS3 and LS8) did not reveal any specific mutation in either the earlier or the later sample.

The presence of the A414G mutation described above was confirmed by other methods (Fig. 4). Although not precisely quantifiable, the T414G mutation could be detected when particularly abundant (≥20%), by direct DNA sequencing of the PCR product of DLP6 fragment (estimated proportion 30 to 40% in Fig. 4B), and in all cases—except in one with minimal amount of mutation—by allele-specific termination of primer extension (Fig. 4, C and D) (*29*). The frequencies of the mutation detected by the primer extension method agree with those determined by DGGE-cloning-sequencing, the tendency toward somewhat lower values presumably reflecting a change in secondary structure of the template caused by the AT to CG base-pair mutation at position 414 (Fig. 4D).

The analysis of the DLP4 clones (Fig. 3) (*25*) revealed a T152C transition in two individuals, that is, in 23 and 31%, respectively, of the DLP4 clones from 48 y and 100(2) y. The latter individual also exhibited, in the same 31% of its DLP4 clones, a T146C transition and a T195C transition, while 48 y exhibited in all its clones the T195C transition, presumably an inherited polymorphism. The T → C transitions at positions 146, 152, and 195 were previously described as polymorphisms (*27*). None of the high-frequency base substitutions detected in the DLP4 fragments from the individuals ≥48 years old analyzed here was present in the DLP4 fragments of nine individuals younger than 48 years, as judged from the first-DGGE patterns and from the results of direct DNA sequencing of the PCR-amplified DLP4 fragments (*30*).

The age distribution and the results of the

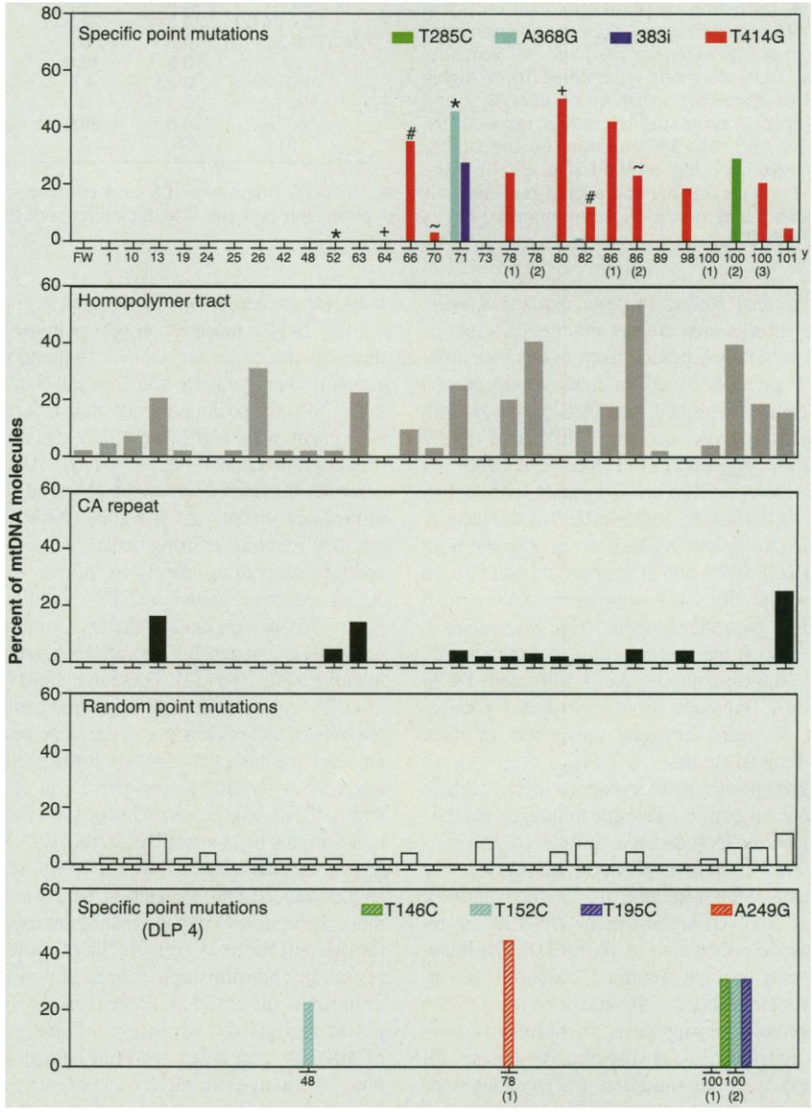

Fig. 3. Diagram summarizing the age distribution and frequency of the various types of heteroplasmic mutations detected in the present work. The upper four panels show the DLP6 mutations, the lowest panel, the DLP4 mutations. The dashes below each abscissae axis indicate the individuals analyzed, with the age in years (fw = 20-week fetal). In the uppermost panel, the two samples of each LS pair are indicated by a distinct symbol (*, +, #, ~).

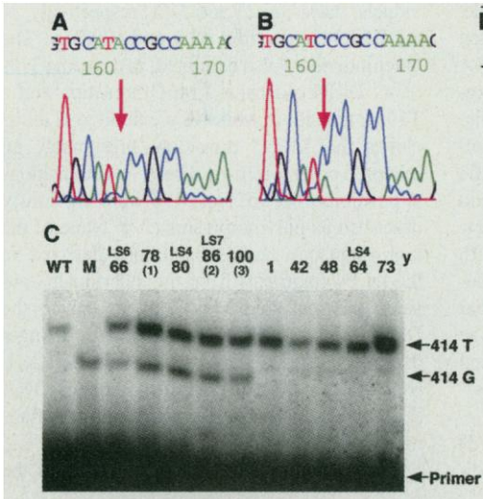

D

Age (y)	DGGE (%)	Primer Extension (%)
20wf	0	0
1	0	0
10	0	0
13	0	0
19	0	0
24	0	0
25	0	0
26	0	0
42	0	0
48	0	0
LS1-52	0	0
LS3-63	0	0
LS4-64	0	0
LS6-66	35.1	23.1
LS7-70	3.4	1.4
LS1-71	0	0
LS8-73	0	0
78 (1)	24.4	20.8
LS3-78 (2)	0	0
LS4-80	50.0	31.7
LS6-82	12.2	3.2
86 (1)	42.2	27.4
LS7-86 (2)	23.3	24.3
LS8-89	0	0
98	18.8	10.0
100 (1)	0	4.5
100 (2)	0	0
100 (3)	20.8	20.4
101	4.5	0

Fig. 4. Detection of T414G (A414C) mutation by DNA sequencing and allele-specific termination of primer extension. [(A) and (B)] Sequences of DLP6 fragments amplified from highly purified fibroblast mtDNAs of LS7-70 y and LS7-86(2) y, estimated to contain, respectively, (**A**) 3% and (**B**) 23% mutation by the DGGE-cloning-sequencing method (Fig. 3). [(C) and (D)] Primer extension data of a representative set of DLP6 fragments (**C**), and comparison of frequencies of mutation determined by the primer extension and the DGGE-cloning-sequencing methods (**D**).

longitudinal studies indicate that the specific base substitutions are not inherited. A role of nuclear mtDNA pseudogenes in this phenomenon is excluded by several lines of evidence: (i) the failure to obtain any PCR products with primers specific for the DLP6 and DLP4 mtDNA segments from total cell DNA of mtDNA-less $\rho^0$206 cells, digested with Bgl II, Dra III, RNase A, and Exo III; (ii) the identity of the DLP6 first-DGGE patterns obtained from total cell DNA and from purified mtDNA of individual fibroblast samples exhibiting such specific base substitutions (Fig. 2A, panels b and c); (iii) the absence of any of the specific base substitutions in the DLP6 and DLP4 mtDNA fragments from individuals younger than 48 years; and (iv) the results of three longitudinal studies.

The specific point mutations identified here may occur during aging due to oxygen radical–induced mtDNA damage, to mtDNA polymerase errors, or to a phenomenon akin to the bacterial SOS response, that is, activation of genes involved in error-prone DNA repair, recently described also in yeast (*31*). The mutation may become amplified, because of an intracellular replicative advantage of the mtDNA molecules carrying them, in fibroblasts from old individuals, as previously shown for pathogenic point mutations (*32*) and deletions (*33*). The cells with amplified mtDNA may then take over the whole population due to their clonal growth advantage. A similar mechanism has recently been proposed for the homoplasmic or near-homoplasmic somatic mutations in human colorectal tumors (*34*).

The T414G transversion occurs in the middle of the promoter for mtDNA H-strand replication primer synthesis and L-strand transcription (LSP), at a position immediately adjacent to a segment with high affinity for the mtTFA transcription factor (Fig. 2D) (*35*). Also the other seven specific mutations observed in old individuals occur at positions critical for mtDNA replication, in particular, either in the coding sequence of the RNA primer for H-strand synthesis, within mtTFA binding segments (*36*), or very close to the O_{H_1} primary site or to the O_{H_2} secondary site of DNA synthesis initiation (Fig. 2D) (*35*). These mutations occur in DNA sequences that either unwind and bend because of mtTFA binding at the same or at an adjacent position (*35, 36*), or form persistent RNA-DNA hybrids giving rise to an R loop with a tRNA-like cloverleaf structure at one or more origins of H-strand synthesis (*37*). These conformational changes would likely expose single-stranded DNA stretches, which may be more susceptible to oxygen radical damage. Although preliminary results have failed to reveal any relationship between any of these mutations and mtDNA content in the fibroblasts, replicative advantage of one subset of mtDNA molecules need not be accompanied by changes in mtDNA content (*32*).

References and Notes

1. A. Harman, *Age* **6**, 86 (1983); A. W. Linnane, S. Marzuki, T. Ozawa, M. Tanaka, *Lancet* **1**, 642 (1989); J. E. Fleming, J. Miquel, S. F. Cottrell, L. S. Yengoyan, A. C. Economos, *Gerontology* **28**, 44 (1982).
2. L. Piko, A. J. Hougham, K. J. Bulpitt, *Mech. Ageing Dev.* **43**, 279 (1988); M. K. Shigenaga, T. M. Hagen, B. N. Ames, *Proc. Natl. Acad. Sci. U.S.A.* **91**, 10771 (1994).
3. N. W. Soong, D. R. Hinton, G. A. Cortopassi, N. Arnheim, *Nature Genet.* **2**, 318 (1992); M. Corral-Debrinski *et al.*, *ibid.*, p. 324; M. Hayakawa, K. Hattori, S. Sugiyama, T. Ozawa, *Biochem. Biophys. Res. Commun.* **189**, 979 (1992).
4. F. Pallotti, X. Chen, E. Bonilla, E. A. Schon, *Am. J. Hum. Genet.* **59**, 591 (1996).
5. G. Attardi, *Int. Rev. Cytol.* **93**, 93 (1985).
6. M. Hasegawa and S. Horai, *J. Mol. Evol.* **32**, 37 (1991); M. Stoneking, D. Hedgecock, R. G. Higuchi, L. Vigilant, H. A. Erlich, *Am. J. Hum. Genet.* **48**, 370 (1991).
7. E. E. Jazin, L. Cavelier, I. Eriksson, L. Oreland, U. Gyllensten, *Proc. Natl. Acad. Sci. U.S.A.* **93**, 12382 (1996).
8. M. Hirano *et al.*, *ibid.* **94**, 14894 (1997); D. C. Wallace, C. Stugard, D. Murdock, T. Schurr, M. D. Brown, *ibid.*, p. 14900.
9. Y. Michikawa, G. Hofhaus, L. S. Lerman, G. Attardi, *Nucleic Acids Res.* **25**, 2455 (1997).
10. M. P. King and G. Attardi, *Science* **246**, 500 (1989).
11. Y. Michikawa, unpublished observations. The methods used are available at (*38*).
12. B. D. Greenberg, J. E. Newbold, A. Sugino, *Gene* **21**, 33 (1983).
13. M. W. Walberg and D. A. Clayton, *Nucleic Acids Res.* **9**, 5411 (1981).
14. J. Montoya, T. Christianson, D. Levens, M. Rabinowitz, G. Attardi, *Proc. Natl. Acad. Sci. U.S.A.* **79**, 7195 (1982).
15. W. W. Hauswirth and D. A. Clayton, *Nucleic Acids Res.* **13**, 8093 (1985).
16. S. Anderson *et al.*, *Nature* **290**, 457 (1981).
17. D. R. Marchington, G. M. Hartshorne, D. Barlow, J. Poulton, *Am. J. Hum. Genet.* **60**, 408 (1997).
18. See (*38*) for methods used for total DNA and mtDNA isolation.
19. See (*38*) for primers used and details about the PCR amplification.
20. As shown in Fig. 1C, before the enzyme treatment, the nuclear DNA present in the total cell DNA sample migrated in an agarose gel as a band moving more slowly than the 23.1-kb λ DNA Hind III fragment, and the heterogeneous RNA migrated faster than the 2-kb λ DNA fragment. After the three digestion steps, no ethidium bromide–stained material was recognizable in the gel.
21. Skin fibroblasts from normal Caucasian individuals were either obtained from the NIGMS Human Genetic Mutant Cell Repository (Camden, NJ) (20 wf, 1 y, 10 y, 13 y, 19 y, 24 y, 25 y, 26 y, 42 y, 48 y, 78-1 y, 98 y), or from the National Institute of Aging Cell Respository (Camden, NJ) {nine twice-sampled longitudinal study (LS) individuals [LS1 (52 y–71 y), LS2 (59 y–75 y), LS3 (63 y–78-2 y), LS4 (64 y–80 y), LS5 (65 y–74-1 y), LS6 (66 y–82 y), LS7 (70 y–86-2 y), LS8 (73 y–89 y), LS9 (77 y–90 y)] and 74-2 y}, or from the Institute of Clinical Neurology of the University of Milan, Italy (86-1 y, 100-1 y, 100-2 y, 100-3 y, 101 y). The latter set of individuals, all from retirement homes, were free of any neurological or muscular pathology. All fibroblast cultures had undergone less than 10 passages when received, and were in general used within two or three additional passages.
22. See (*38*) for methods for fibroblast culture and first DGGE analysis.
23. Methods for mtDNA cloning and second-DGGE analysis can be found in (*38*).
24. The method for sequencing is described in (*38*).
25. A table summarizing the sequence data obtained for the cloned DLP6 and DLP4 fragments analyzed in this work is available at (*38*).
26. A cloned wild-type DLP6 mtDNA fragment from the 25-year-old individual and a cloned wild-type DLP4 mtDNA fragment from the 78-year-old individual were PCR reamplified, and the recloned PCR products, and 48 cloned fragments thus isolated were then subjected to a second DGGE screening.
27. A. M. Kogelnik, M. T. Lott, M. D. Brown, S. B. Navathe, D. C. Wallace, *Nucleic Acids Res.* **26**, 112 (1998).
28. A repeat of the cloning and sequencing of the DLP6 fragments of the two LS6 samples gave results that, when combined with the previous ones, yielded a co-

efficient of variation for the frequency of the specific point mutations of ~20%, supporting the reproducibility of the estimates. Therefore, it is possible that the observed decrease in the T414G mutation frequency in the LS6-82 y sample results from a difference in the biopsy site or from handling of the original specimen.
29. The method for allele-specific termination of primer extension is described in (38).
30. Y. Michikawa and G. Attardi, data not shown.
31. N. B. Reuven, G. Tomer, Z. Livneh, *Mol. Cell* **2**, 191 (1998).
32. M. Yoneda, A. Chomyn, A. Martinuzzi, O. Hurko, G. Attardi, *Proc. Natl. Acad. Sci. U.S.A.* **89**, 11164 (1992).
33. N.-G. Larsson, E. Holme, B. Kristiansson, A. Oldfors, M. Tulinius, *Pediatr. Res.* **28**, 131 (1990).
34. K. Polyak *et al.*, *Nature Genet.* **20**, 291 (1998).
35. S. C. Ghivizzani, C. S. Madsen, M. R. Nelen, C. V. Ammini, W. W. Hauswirth, *Mol. Cell. Biol.* **14**, 7717 (1994).
36. R. P. Fisher, T. Lisowsky, M. A. Parisi, D. A. Clayton, *J. Biol. Chem.* **267**, 3358 (1992).
37. D. Y. Lee and D. A. Clayton, *Genes Dev.* **11**, 582 (1997); *J. Biol. Chem.* **273**, 30614 (1998).
38. Supplemental material is available at the *Science* Web site (www.sciencemag.org/feature/data/1040395.shl).
39. Supported by National Institute on Aging (NIH) grant AG12117-03 (to G.A.). We thank A. Chomyn and G. Villani for valuable discussions, M. Lai for support, A. Aman, R. Steinberger, and M. Scott for their help with experiments, and A. Drew, B. Keeley, R. Zedan, and C. Lin for expert technical assistance.

26 March 1999; accepted 14 September 1999

Crystal Structure of the Ectodomain of Human Transferrin Receptor

C. Martin Lawrence,[1,2] Sanjoy Ray,[1]* Marina Babyonyshev,[1] Renate Galluser,[1] David W. Borhani,[1]† Stephen C. Harrison[1,2]‡

The transferrin receptor (TfR) undergoes multiple rounds of clathrin-mediated endocytosis and reemergence at the cell surface, importing iron-loaded transferrin (Tf) and recycling apotransferrin after discharge of iron in the endosome. The crystal structure of the dimeric ectodomain of the human TfR, determined here to 3.2 angstroms resolution, reveals a three-domain subunit. One domain closely resembles carboxy- and aminopeptidases, and features of membrane glutamate carboxypeptidase can be deduced from the TfR structure. A model is proposed for Tf binding to the receptor.

The transferrin receptor (TfR) assists iron uptake into vertebrate cells through a cycle of endo- and exocytosis of the iron transport protein transferrin (Tf) (*1*). TfR binds iron-loaded (diferric) Tf at the cell surface and carries it to the endosome. Iron dissociates from Tf upon acidification of the endosome, but apo-Tf remains tightly bound to TfR. The complex then returns to the cell surface. At extracellular pH, apo-Tf dissociates and is replaced by diferric Tf from serum. This cycle has become one of the most widely studied models for receptor-mediated endocytosis.

Human TfR is a homodimeric type II transmembrane protein. The 90-kD subunit has a short, NH_2-terminal cytoplasmic region (residues 1 to 67), which contains the internalization motif YTRF (*2*), a single transmembrane pass (residues 68 to 88), and a large extracellular portion (ectodomain, residues 89 to 760), which contains a binding site for the 80-kD Tf molecule. Electron cryomicroscopy shows that the TfR dimer has a globular, extracellular structure separated from the membrane by a stalk of about 30Å (*3*). The stalk presumably includes residues immediately following the transmembrane pass and the O-linked glycan at Thr^{104} [see (*4*) and references therein] as well as two intermolecular disulfide bonds—one formed by Cys^{89} and one formed by Cys^{98} (*5*). The intermolecular disulfides are not required for dimerization (*6*). Treatment of TfR-containing membranes with trypsin releases a soluble fragment, residues 121 to 760, whose crystallization has been described (*7*). The released receptor is a dimer. It binds two molecules of Tf with normal affinity and it corresponds to the large globular structure shown by electron microscopy. A similar fragment is found as a normal component of human serum; its level is inversely correlated with body iron stores (*4*). HFE, the product of the gene responsible for human hereditary hemochromatosis (tissue iron overload) and a homolog of the heavy chain of class I major histocompatibility complex molecules, has recently been identified as a second ligand for TfR (*8*). Hereditary hemochromatosis is the most common genetic disease among persons of northern European descent. Association with HFE lowers the affinity of TfR for Tf by a factor of 10 to 50 (*8*) and also appears to impede dissociation of iron from Tf in the endosome (*9*).

The amino acid sequence of the globular ectodomain of TfR is 28% identical to that of membrane glutamate carboxypeptidase II (mGCP). mGCP hydrolyzes *N*-acetyl-α-L-aspartyl-L-glutamate, the most prevalent mammalian neuropeptide (*10*). Several groups have noticed the similarity of mGCP to aminopeptidases, and one group has extended this analysis to TfR, suggesting that TfR evolved from a peptidase related to mGCP (*11*). In TfR, three of the presumed Zn ligands of the predicted protease-like domain are missing, and TfR lacks peptidase activity.

We have expressed an equivalent of the tryptic fragment of human TfR in Chinese hamster ovary (CHO) cells (*12*) and determined its structure at 3.2 Å resolution (*13*). Because crystals of TfR diffract significantly better after soaking in $SmCl_3$, we determined the structure of TfR in the presence of bound Sm^{3+} ions. The asymmetric unit of the crystals contains four TfR dimers (8 × 70 kD = 560 kD) stacked in an 8_5 helical array coincident with a crystallographic 2_1 axis (*14*). We have found interpretable electron density for the entire tryptic fragment except for Arg^{121} at the NH_2-terminus. We also see density for the first *N*-acetylglucosamine residue at each of the three N-linked glycosylation sites (*15*).

The TfR monomer contains three distinct domains, organized so that the TfR dimer has a butterfly-like shape (Fig. 1). The positions of the NH_2-termini allow orientation of TfR with respect to the plasma membrane. Secondary structural elements for each domain are shown in Fig. 2; the notation used below is explained in the legend. The first, protease-like domain contains residues 122 through 188 and 384 through 606. Its fold, which is closely related to that of carboxy- or aminopeptidase (*16*), has a central, seven-stranded, mixed β sheet with flanking α helices (Fig. 2A). Carboxypeptidase itself has eight β strands, but in TfR the polypeptide chain traces a path away from the outside edge of the β sheet, forming an extended loop (α1–7/α1–8). A disulfide bond within the protease-like domain is unusual in linking Cys^{556} and Cys^{558}, only two residues apart at the end of βI-6.

The second, apical domain contains residues 189 to 383. It resembles a β sandwich in which the two sheets are splayed apart (Fig. 2B), with a helix (αII-2) running along the open edge. A related structure has been seen in domain 4 of aconitase (*17*). An extended segment of polypeptide connects βII-6 and βII-7, traversing the interface between the apical and protease-like domains. At the COOH-terminus of this apical traverse is a

[1]Howard Hughes Medical Institute and Children's Hospital Laboratory of Molecular Medicine, 320 Longwood Avenue, Boston, MA 02115, USA. [2]Department of Biological Chemistry and Molecular Pharmacology, Harvard Medical School, Boston, MA 02115, USA.

*Present address: Whitehead Institute, 9 Cambridge Center, Cambridge, MA 02142, USA.
†Present address: Department of Organic Chemistry, 2000 Ninth Avenue South, Southern Research Institute, Birmingham, AL 35205, USA.
‡To whom correspondence should be addressed. E-mail: harrison@crystal.harvard.edu

http://www.jstor.org

LINKED CITATIONS

- Page 1 of 2 -

You have printed the following article:

Aging-Dependent Large Accumulation of Point Mutations in the Human mtDNA Control Region for Replication

Yuichi Michikawa; Franca Mazzucchelli; Nereo Bresolin; Guglielmo Scarlato; Giuseppe Attardi

Science, New Series, Vol. 286, No. 5440. (Oct. 22, 1999), pp. 774-779.

Stable URL:

http://links.jstor.org/sici?sici=0036-8075%2819991022%293%3A286%3A5440%3C774%3AALAOPM%3E2.0.CO%3B2-F

This article references the following linked citations:

References and Notes

[2] **Oxidative Damage and Mitochondrial Decay in Aging**

Mark K. Shigenaga; Tory M. Hagen; Bruce N. Ames

Proceedings of the National Academy of Sciences of the United States of America, Vol. 91, No. 23. (Nov. 8, 1994), pp. 10771-10778.

Stable URL:

http://links.jstor.org/sici?sici=0027-8424%2819941108%2991%3A23%3C10771%3AODAMDI%3E2.0.CO%3B2-3

[7] **Human Brain Contains High Levels of Heteroplasmy in the Noncoding Regions of Mitochondrial DNA**

Elena E. Jazin; Lucia Cavelier; Inger Eriksson; Lars Oreland; Ulf Gyllensten

Proceedings of the National Academy of Sciences of the United States of America, Vol. 93, No. 22. (Oct. 29, 1996), pp. 12382-12387.

Stable URL:

http://links.jstor.org/sici?sici=0027-8424%2819961029%2993%3A22%3C12382%3AHBCHLO%3E2.0.CO%3B2-L

[8] **Apparent mtDNA Heteroplasmy in Alzheimer's Disease Patients and in Normals Due to PCR Amplification of Nucleus-Embedded mtDNA Pseudogenes**

Michio Hirano; Alexander Shtilbans; Richard Mayeux; Mercy M. Davidson; Salvatore DiMauro; James A. Knowles; Eric A. Schon

Proceedings of the National Academy of Sciences of the United States of America, Vol. 94, No. 26. (Dec. 23, 1997), pp. 14894-14899.

Stable URL:

http://links.jstor.org/sici?sici=0027-8424%2819971223%2994%3A26%3C14894%3AAMHIAD%3E2.0.CO%3B2-B

NOTE: *The reference numbering from the original has been maintained in this citation list.*

http://www.jstor.org

LINKED CITATIONS

[10] **Human Cells Lacking mtDNA: Repopulation with Exogenous Mitochondria by Complementation**

Michael P. King; Giuseppe Attardi

Science, New Series, Vol. 246, No. 4929. (Oct. 27, 1989), pp. 500-503.

Stable URL:

http://links.jstor.org/sici?sici=0036-8075%2819891027%293%3A246%3A4929%3C500%3AHCLMRW%3E2.0.CO%3B2-A

[14] **Identification of Initiation Sites for Heavy-Strand and Light-Strand Transcription in Human Mitochondrial DNA**

Julio Montoya; Thomas Christianson; David Levens; Murray Rabinowitz; Giuseppe Attardi

Proceedings of the National Academy of Sciences of the United States of America, Vol. 79, No. 23, [Part 1: Biological Sciences]. (Dec. 1, 1982), pp. 7195-7199.

Stable URL:

http://links.jstor.org/sici?sici=0027-8424%2819821201%2979%3A23%3C7195%3AIOISFH%3E2.0.CO%3B2-5

[32] **Marked Replicative Advantage of Human mtDNA Carrying a Point Mutation that Causes the MELAS Encephalomyopathy**

Makoto Yoneda; Anne Chomyn; Andrea Martinuzzi; Orest Hurko; Giuseppe Attardi

Proceedings of the National Academy of Sciences of the United States of America, Vol. 89, No. 23. (Dec. 1, 1992), pp. 11164-11168.

Stable URL:

http://links.jstor.org/sici?sici=0027-8424%2819921201%2989%3A23%3C11164%3AMRAOHM%3E2.0.CO%3B2-3

NOTE: *The reference numbering from the original has been maintained in this citation list.*